Tunable resonant radiation force exerted on semiconductor quantum well nanostructures: Nonlocal effects*

Guang-Hui Wang(王光辉)[1,2,†], Xiong-Shuo Yan(颜雄硕)[1,2], and Jin-Ke Zhang(张金珂)[1,2]

[1] *Guangzhou Key Laboratory for Special Fiber Photonic Devices, South China Normal University, Guangzhou* 510006, *China*

[2] *Guangdong Provincial Key Laboratory of Nanophotonic Functional Materials and Devices, South China Normal University, Guangzhou* 510006, *China*

(Received 27 March 2017; revised manuscript received 3 July 2017; published online 20 August 2017)

Resonant radiation force exerted on a semiconductor quantum well nanostructure (QWNS) from intersubband transition of electrons is investigated by taking the nonlocal coupling between the polarizability of electrons and applied optical fields into account for two kinds of polarized states. The numerical results show the spatial nonlocality of optical response can induce the spectral peak position of the exerted force to have a blueshift, which is sensitively dependent on the polarized state and the QWNS width. It is also demonstrated that resonant radiation force is controllable by the polarization and incident directions of applied light waves. This work provides effective methods for controlling optical force and manipulating nano-objects, and observing radiation forces in experiment. This nonlocal interaction mechanism can also be used to probe and predominate internal quantum properties of nanostructures, and to manipulate collective behavior of nano-objects.

Keywords: nonlocal effect, radiation force, quantum well, nanostructure

PACS: 68.65.Fg, 11.10.Lm, 45.20.da **DOI:** 10.1088/1674-1056/26/10/106802

1. Introduction

Optical force and optical manipulation of nano-objects have been attracting extensive research interest since the trapping of dielectric particles was proposed by Ashkin and associates in 1986.[1] Many fruitful research results have been reported and have extensive potential applications in various fields such as physics, biology, engineering dynamics, and so on.[2–10] For example, Chaumet and Nieto-Vesperinas studied optical force exerted on a dipolar sphere by an electromagnetic field, and established the time-averaged total force on a subwavelength-sized particle in a time-harmonic-varying field.[9]

At present, there has also been an increase of interest in nonlocal optical response of semiconductor and metal nanostructures.[11–17] The so-called nonlocal optical response is that the polarization at a spatial point is induced by the applied optical fields not only at the same point, but also at other positions within the extent of the relevant wave function of electrons. Consequently, dielectric permittivity of nonlocal materials is not only the function of frequency, but also the function of wavevector in the spectral domain. Since the pioneer theoretical work of Pekar on spatial nonlocality in semiconductor bulk materials,[18] the theoretical work has been developed further towards nanostructures by Cho[19] and towards metamaterials by Belov.[20] Some novel nonlocal effects have also been observed in thin GaAs layers by Ishihara,[21] and in metamaterials by Luukkonen.[22] The nonlocal optical effects in the mesoscopic systems have been drawing more and more attention, giving rise to the development of nonlocal theory and nonlocal optical properties in plasmon and semiconductor nanostructures.[23–25] In 2009, McMahon *et al.*[17] investigated nonlocal optical response of metal nanostructures with an arbitrary shape, and demonstrated that nonlocal effect induces an evident blueshift at the plasmon resonance in absorption spectra and it is particularly important in apex structures. In 2013, Luo *et al.*[25] proposed a simple model for dealing with the nonlocality of optical response in metallic nanoparticles. To our knowledge, the effects of spatial nonlocality of optical response on optical force are not clarified. It is possible and desirable, however, that the nonlocal effects may have important influence on optical force exerted on nano-objects. The physical motive of our paper is to investigate and clarify how the nonlocal effects influence optical force exerted on a quantum well nanostructure (QWNS) from the resonant intersubband transitions for two different polarized states.

This paper is organized as follows. In Section 2, a basic theoretical framework for optical force exerted on a QWNS from resonant intersubband transitions for two different polarized states is presented by taking spatial nonlocality of optical response into account. In Section 3, the numerical results and discussion are presented for a AlGaAs/GaAs QWNS. These results show that the spatial nonlocality of optical response has evident influence on optical force spectra. Brief conclusions are given in Section 4.

*Project supported by the National Natural Science Foundation of China (Grant No. 11474106), the Natural Science Foundation of Guangdong Province, China (Grant No. 2016A030313439), and the Science and Technology Program of Guangzhou City, China (Grant No. 201707010403).

†Corresponding author. E-mail: wanggh@scnu.edu.cn

© 2017 Chinese Physical Society and IOP Publishing Ltd

2. Theoretical framework for optical force on a QWNS with nonlocal response

Let us consider that a monochromatic plane wave is incident on a square QWNS with an incident angle θ and angular frequency ω in the two cases of p- and s-polarized states, as shown in Fig. 1. The square QWNS of the width L is confined in the z direction. Two surfaces of the QWNS are located at xy plane with $z=0$ and $z=L$, respectively. It is well known that the Lorentz force on charged particles in an electromagnetic field is generally described as[26]

$$F(t)=\int_V[\rho(\boldsymbol{r},t)\boldsymbol{E}(\boldsymbol{r},t)+\boldsymbol{j}(\boldsymbol{r},t)\times\boldsymbol{B}(\boldsymbol{r},t)]\,\mathrm{d}\boldsymbol{r}, \quad (1)$$

where $\boldsymbol{E}(\boldsymbol{r},t)$ and $\boldsymbol{B}(\boldsymbol{r},t)$ are the electric and magnetic fields, respectively. $\rho(\boldsymbol{r},t)$ is the charge density, and $\boldsymbol{j}(\boldsymbol{r},t)$ is the current density. V is the volume of the loaded body. By using $\rho(\boldsymbol{r},t)=-\nabla\boldsymbol{P}(\boldsymbol{r},t)$, and

$$\int_V[\nabla\cdot\boldsymbol{P}(\boldsymbol{r},t)]\boldsymbol{E}(\boldsymbol{r},t)\,\mathrm{d}\boldsymbol{r}=-\int_V[\boldsymbol{P}(\boldsymbol{r},t)\cdot\nabla]\boldsymbol{E}(\boldsymbol{r},t)\,\mathrm{d}\boldsymbol{r},$$

where $\boldsymbol{P}(\boldsymbol{r},t)$ is the induced polarization, one can derive the time-averaged radiation force on the QWNS per unit area as

$$\langle\boldsymbol{F}\rangle(\omega)=\int_V\int_{-T/2}^{T/2}\frac{\mathrm{d}\boldsymbol{r}\,\mathrm{d}t}{TS}[\boldsymbol{P}(\boldsymbol{r},t)\cdot\nabla\boldsymbol{E}(\boldsymbol{r},t)+\dot{\boldsymbol{P}}(\boldsymbol{r},t)\times\boldsymbol{B}(\boldsymbol{r},t)], \quad (2)$$

where T denotes one oscillation period of incident electromagnetic fields, S is the surface area of the QWNS, respectively. $\dot{\boldsymbol{P}}$ denotes the one-order derivation of time for $\boldsymbol{P}(\boldsymbol{r},t)$. For time harmonic electromagnetic fields, we can write

$$\begin{aligned}\boldsymbol{E}(\boldsymbol{r},t)&=\mathrm{Re}\{\boldsymbol{E}(\boldsymbol{r},\omega)\exp(-\mathrm{i}\omega t)\},\\ \boldsymbol{B}(\boldsymbol{r},t)&=\mathrm{Re}\{\boldsymbol{B}(\boldsymbol{r},\omega)\exp(-\mathrm{i}\omega t)\},\\ \boldsymbol{P}(\boldsymbol{r},t)&=\mathrm{Re}\{\boldsymbol{P}(\boldsymbol{r},\omega)\exp(-\mathrm{i}\omega t)\},\end{aligned}$$

$\boldsymbol{E}(\boldsymbol{r},\omega)$, $\boldsymbol{B}(\boldsymbol{r},\omega)$, and $\boldsymbol{P}(\boldsymbol{r},\omega)$ are complex functions of position and frequency. Re denotes the real part. On performing the integral and using $\boldsymbol{B}(\boldsymbol{r},\omega)=1/(\mathrm{i}\omega)\nabla\times\boldsymbol{E}(\boldsymbol{r},\omega)$, one can obtain further the time-averaged force on the QWNS per unit area as[6,9]

$$\langle\boldsymbol{F}\rangle(\omega)=\frac{1}{2S}\mathrm{Re}\left\{\int_V\mathrm{d}\boldsymbol{r}\bigtriangledown\boldsymbol{E}(\boldsymbol{r},\omega)^*\cdot\boldsymbol{P}(\boldsymbol{r},\omega)\right\}, \quad (3)$$

where * denotes the complex conjugate. In the case of nonlocal linear response, the resonant part of the induced polarization is microscopically described as

$$\boldsymbol{P}(\boldsymbol{r},\omega)=\varepsilon_0\int_V\overline{\overline{\chi}}(\boldsymbol{r},\boldsymbol{r}';\omega)\cdot\boldsymbol{E}(\boldsymbol{r}',\omega)\,\mathrm{d}\boldsymbol{r}',$$

where $\overline{\overline{\chi}}(\boldsymbol{r},\boldsymbol{r}';\omega)$ is the nonlocal susceptibility tensor. Due to the system with the translational invariance in the x direction and the confinement in the z direction, the complex electric field $\boldsymbol{E}(\boldsymbol{r},\omega)$ and the complex polarization $\boldsymbol{P}(\boldsymbol{r},\omega)$ can be assumed to have the forms $\boldsymbol{E}(\boldsymbol{r},\omega)=\widetilde{\boldsymbol{E}}(z;\omega)\exp(\mathrm{i}k_x x)$ and $\boldsymbol{P}(\boldsymbol{r},\omega)=\widetilde{\boldsymbol{P}}(z;\omega)\exp(\mathrm{i}k_x x)$, where k_x stands for the wave number in the x direction. By the density-matrix method as mentioned in Ref. [11], the components of the complex amplitudes of the linear polarization, $\widetilde{\boldsymbol{P}}(z,\omega)$, for the two-level QWNS model can be obtained as follows:

$$\widetilde{P}_j(z,\omega)=-\frac{\mathrm{e}^2}{2\pi\hbar^2\omega^2}\frac{(\varepsilon_F-\varepsilon_1)^2N_j\Psi(z)}{\hbar\omega-\varepsilon_{21}+\mathrm{i}\hbar\Gamma_0},\ (j=x,y), \quad (4)$$

$$\widetilde{P}_z(z,\omega)=\frac{\mathrm{e}^2}{4\pi m^*\omega^2}\frac{(\varepsilon_1-\varepsilon_F)N_z\zeta(z)}{\hbar\omega-\varepsilon_{21}+\mathrm{i}\hbar\Gamma_0}, \quad (5)$$

where

$$N_j\equiv\int_0^L\Psi(z)\widetilde{E}_j(z;\omega)\,\mathrm{d}z,\ \ N_z\equiv\int_0^L\zeta(z)\widetilde{E}_z(z;\omega)\,\mathrm{d}z.$$

$$\Psi(z)=\varphi_1(z)\varphi_2(z),\ \ \zeta(z)=\varphi_1(z)\frac{\mathrm{d}\varphi_2(z)}{\mathrm{d}z}-\varphi_2(z)\frac{\mathrm{d}\varphi_1(z)}{\mathrm{d}z},$$

with $\varphi_n(z)=\sqrt{2/L}\sin(n\pi z/L)$ and $\varepsilon_n=n^2\pi^2\hbar^2/(2m^*L^2)$ $(n=1,2)$ are the envelope wave functions and the transverse energies of the n-th subband of the two-level QWNS, respectively.[27] m^* is the effective mass of an electron in conduction bands. e is the electron charge. Γ_0 is the non-radiation relaxation rate. $\hbar\Gamma_0$ is called the relaxation energy. $\varepsilon_{21}=\varepsilon_2-\varepsilon_1$ is the level spacing between ε_2 and ε_1. $\varepsilon_F=\varepsilon_1+\pi N_s\hbar^2/m^*$ is the Fermi energy of the QWNS system, where N_s is the donor surface concentration. From the expressions of N_j and N_z, we can see that the nonlocal optical response makes the polarization at a certain point in space to be induced by the applied optical fields not only at the same point, but also at other positions within the extent of the relevant wave functions in the QWNS.

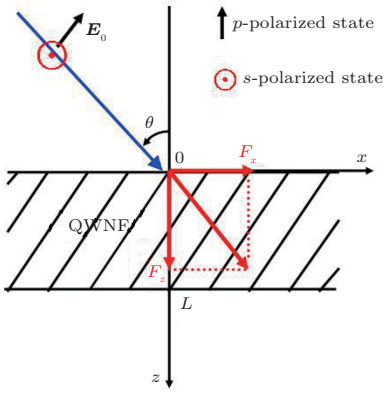


Fig. 1. (color online) The schematic diagrams of a QWNS, radiation forces, and incident and polarization direction of a monochromatic plane wave. F_x and F_z denote the x and z components of the radiation force exerted on the QWNS by incident light, respectively. The signs ↑ and ⊙ denote polarization direction of p- and s-polarized light waves, respectively.

By the Green's function method,[11,19] one can solve the components of the microscopic electric field ($\widetilde{E}_y$ for s-polarized state, $\widetilde{E}_x$ and $\widetilde{E}_z$ for p-polarized state) from Maxwell's equations, satisfying the self-consistent integral equations[15]

$$\widetilde{E}_y(z;\omega) = \widetilde{E}_{0y}(z;\omega) + \frac{\alpha N_y}{2\mathrm{i}k_\perp}\int_0^L \mathrm{e}^{\mathrm{i}k_\perp|z-z'|}\Psi(z')\,\mathrm{d}z', \quad (6)$$

$$\widetilde{E}_x(z;\omega) = \widetilde{E}_{0x}(z;\omega) + \alpha N_x\int_0^L G_{xx}(z,z';\omega)\Psi(z')\,\mathrm{d}z' + \beta N_z\int_0^L G_{xz}(z,z';\omega)\zeta(z')\,\mathrm{d}z', \quad (7)$$

$$\widetilde{E}_z(z;\omega) = \widetilde{E}_{0z}(z;\omega) + \alpha N_x\int_0^L G_{zx}(z,z';\omega)\Psi(z')dz' + \beta N_z\int_0^L G_{zz}(z,z';\omega)\zeta(z')\,\mathrm{d}z', \quad (8)$$

where $\widetilde{\boldsymbol{E}}_0(z;\omega) = \widetilde{\boldsymbol{E}}_0\exp(\mathrm{i}k_\perp z)$ is the incident field, and $k_\perp = (\varepsilon_b\omega^2/c^2 - k_x^2)^{1/2}$ is the wave-number in the z direction. In addition, $\alpha = \mu_0\mathrm{e}^2(\varepsilon_F-\varepsilon_1)^2/(2\pi\hbar^2\Lambda)$, and $\beta = \mu_0\mathrm{e}^2(\varepsilon_F-\varepsilon_1)/(4\pi m^*\Lambda)$, where $\Lambda = \hbar\omega - \varepsilon_{21} + \mathrm{i}\hbar\Gamma_0$. $G_{ij}(z,z';\omega)$ $(i,j=x,z)$ are the elements of the tensorial Green's function $\overline{\overline{\boldsymbol{G}}}(z,z';\omega)$ of the quantum system[11]

$$\overline{\overline{\boldsymbol{G}}}(z,z';\omega) = \frac{k_x c^2\,\mathrm{e}^{\mathrm{i}k_\perp|z-z'|}}{2\mathrm{i}\varepsilon_b\omega^2}\begin{pmatrix} k_\perp/k_x & \mathrm{sgn}(z'-z) \\ \mathrm{sgn}(z'-z) & k_x/k_\perp\end{pmatrix} + \frac{\delta(z'-z)c^2}{\varepsilon_\mathrm{b}\omega^2}\hat{\boldsymbol{e}}_z\hat{\boldsymbol{e}}_z, \quad (9)$$

where ε_b is the relative dielectric constant for the background medium. $\hat{\boldsymbol{e}}_z$ denotes the unit vector in the z direction. $\mathrm{sgn}(z)$ is the sign function. By multiplying both sides of Eqs. (6), (7), and (8) by $\Psi(z)$ and $\zeta(z)$ respectively, and integrating the three equations over z across the QWNS, one can obtain

$$N_y = \widetilde{S}_y/(1-\alpha M_{yy}), \quad (10)$$

$$N_x = \frac{\widetilde{S}_x(1-\beta M_{zz}) + \beta\widetilde{S}_z M_{xz}}{(1-\alpha M_{xx})(1-\beta M_{zz}) - \alpha\beta M_{xz}M_{zx}}, \quad (11)$$

$$N_z = \frac{\widetilde{S}_z(1-\alpha M_{xx}) + \alpha\widetilde{S}_x M_{zx}}{(1-\alpha M_{xx})(1-\beta M_{zz}) - \alpha\beta M_{xz}M_{zx}}, \quad (12)$$

where

$$M_{xx} = \iint_0^L \Psi(z)G_{xx}(z,z';\omega)\Psi(z')\,\mathrm{d}z\mathrm{d}z',$$

$$M_{yy} = \frac{1}{2\mathrm{i}k_\perp}\iint_0^L \Psi(z)\,\mathrm{e}^{\mathrm{i}k_\perp|z-z'|}\Psi(z')\,\mathrm{d}z\mathrm{d}z',$$

$$M_{xz} = -M_{zx} = \iint_0^L \Psi(z)G_{xz}(z,z';\omega)\zeta(z')\,\mathrm{d}z\mathrm{d}z',$$

$$M_{zz} = \iint_0^L \zeta(z)G_{zz}(z,z';\omega)\zeta(z')\,\mathrm{d}z\mathrm{d}z',$$

$$\widetilde{S}_j = \int_0^L \widetilde{E}_{0j}(z;\omega)\Psi(z)\,\mathrm{d}z, \quad (j=x,y),$$

$$\widetilde{S}_z = \int_0^L \widetilde{E}_{0z}(z;\omega)\zeta(z)\,\mathrm{d}z.$$

For the following analyses, we write Eqs. (10)–(12) into the following matrix form by the rotating wave approximation[19]

$$\overline{\overline{\boldsymbol{D}}}\cdot\widetilde{\boldsymbol{N}} = \widetilde{\boldsymbol{S}}, \quad (13)$$

where $\overline{\overline{\boldsymbol{D}}}$ is a 3×3 diagonal matrix with the following three elements

$$D_{xx} = \hbar\omega - \varepsilon_{21} + \mathrm{i}\hbar\Gamma_0 + hM_{xx},$$
$$D_{yy} = \hbar\omega - \varepsilon_{21} + \mathrm{i}\hbar\Gamma_0 + hM_{yy},$$
$$D_{zz} = \hbar\omega - \varepsilon_{21} + \mathrm{i}\hbar\Gamma_0 + tM_{zz}.$$

The vectors $\widetilde{\boldsymbol{S}} = (\widetilde{S}_x,\widetilde{S}_y,\widetilde{S}_z)$ and $\widetilde{\boldsymbol{N}} = g(N_x,N_y,N_z)$. Here $g = 1/(\hbar\omega-\varepsilon_{21}+\mathrm{i}\hbar\Gamma_0)$, $h = -\mu_0 e^2(\varepsilon_F-\varepsilon_1)^2/(2\pi\hbar^2)$, and $t = \mu_0 e^2(\varepsilon_1-\varepsilon_F)/(4\pi m^*)$. From Eq. (13), it is not hard to see that the resonance structures of the optical force spectra are determined by the complex roots of $\det|\overline{\overline{\boldsymbol{D}}}| = 0$. From the expressions of D_{xx}, D_{yy}, and D_{zz}, we can see that the resonance peak of the radiation force does not occur at $\hbar\omega = \varepsilon_{21}$, but has a shift relative to the level spacing ε_{21}, which is attributed to the contributions from the real part of the three terms hM_{xx}, hM_{yy}, and tM_{zz}, respectively. This kind of shift of resonance peak is called radiation shift.[19] In the expressions of M_{xx}, M_{yy} and M_{zz}, it is evident that the radiative shift of the resonance peak is associated closely with the coupling between the dynamical variables, i.e., the microscopic current-density flows accompanying the change in the wave functions via the electromagnetic propagator $\overline{\overline{\boldsymbol{G}}}(z,z';\omega)$, originating from the nonlocal optical response of electrons to optical fields.

3. Results and discussion

In the following, we analyze optical force exerted on the QWNS by taking spatial nonlocality of optical response into account in detail. Some parameters used in the following calculation are adopted as:[14,15] $m^* = 0.067m_0$ (m_0 is the mass of a free electron), $N_\mathrm{s} = 10^{11}$ cm^{-2}, $\varepsilon_\mathrm{b} = 13.1$, and $\hbar\Gamma_0 = 4.7$ meV. The incident intensity is assumed to be 0.05 W/cm^2. Figure 2 shows the resonant radiation force as a function of the normalized photon energy $\hbar\omega/\varepsilon_{21}$ in the two cases: (a) p-polarization and (b) s-polarization for three different QWNS widths: 5 nm (black lines), 25 nm (red lines), and 40 nm (blue lines) with the incident angle $\theta = 45^\circ$, respectively. F_x and F_z denote the x and z components of the radiation force, respectively. The solid and dashed lines in Fig. 2 correspond to F_z and F_x, respectively, where F_x has been amplified three times for the sake of contrast. It can be seen from Fig. 2 that the resonance peak of the radiation force does not occur at $\hbar\omega = \varepsilon_{21}$, but has a radiative shift relative to the level spacing ε_{21}, originating from the nonlocal optical response. The

nonlocality of optical response in QWNS is enhanced remarkably by the quantum-size effects. The nonlocality of optical response, originating from the coupling between the microscopic current-density flows associated with different spatial points, leads to the coherent extension of the resonantly excited modes of the interacting radiation-matter system. It is worth noting that the radiative shift of F_x is completely the same as that of F_z for a certain polarization state. In addition, the radiative shift is dependent closely on the QWNS width and the polarization direction of incident light, whereas it is not related generally to the angle of incidence.

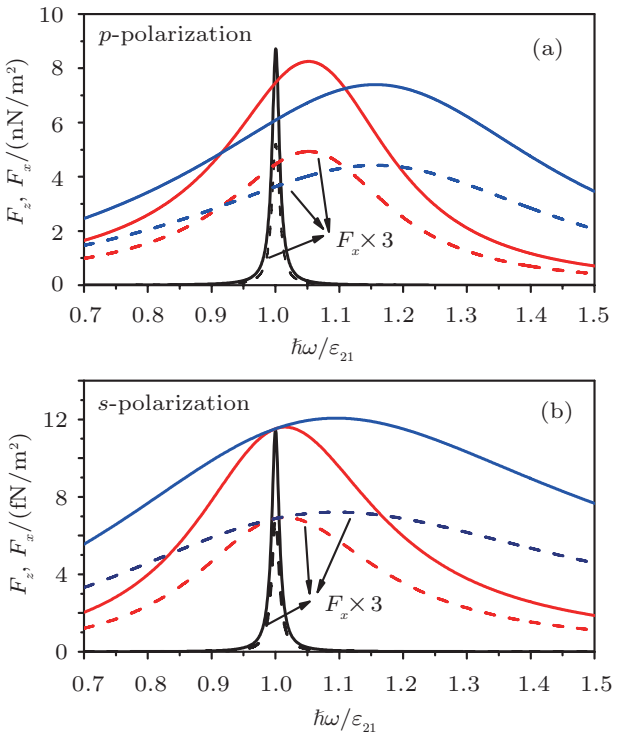


Fig. 2. (color online) Resonant radiation force spectra (F_x: dashed lines; F_z: solid lines) in the two cases of p-polarization (a) and s-polarization (b) for three different QWNS widths: 5 nm (black lines), 25 nm (red lines), and 40 nm (blue lines), respectively.

To see how the QWNS width and the polarized state influence the resonant radiation force spectra, the radiation shift ($\Delta\hbar\omega = \hbar\omega/\varepsilon_{21} - 1$) at resonance is plotted versus the QWNS width L in the two cases of the p- and s-polarizations in Fig. 3. The black, blue, and red-dotted lines correspond to the p-polarization for an incident angle $\theta \neq 0$, s-polarization for an arbitrary θ, and p-polarization for $\theta = 0$, respectively. From Fig. 3, we can see that the radiation shift is a blueshift ($\Delta\hbar\omega > 0$), which is dependent really on the QWNS width and the polarization direction. Specifically speaking, the blueshift increases gradually with increasing the width of the QWNS. The blueshift for p-polarized state excepting $\theta = 0$, however, is more evident and larger than that for s-polarized state generally. This is because there exists the quantum-size effect for p-polarized state when $\theta \neq 0$, which makes the nonlocal effect more evident, whereas there is not the quantum-size effect for s-polarized state. It is worth noting that the resonant radiation force spectrum, including its magnitude and radiative shift, for p-polarization when $\theta = 0$ is completely the same as that for s-polarization. The reason is that the polarization direction is along the x direction for p-polarization when $\theta = 0$, which is equivalent to the y direction for s-polarization. Therefore the variation rules of the blueshift for the two kinds of cases are consistent essentially.

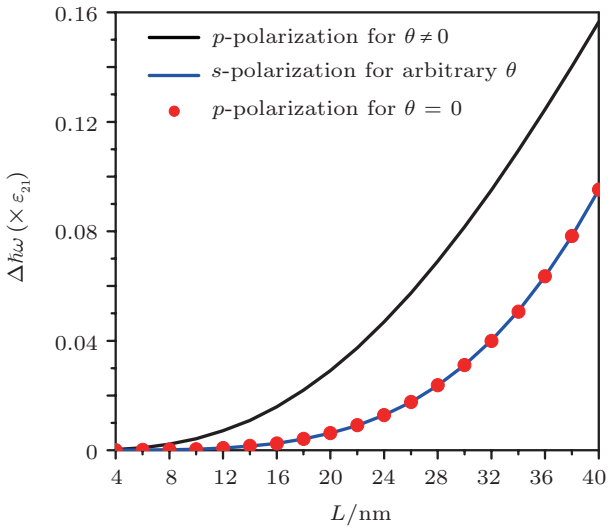


Fig. 3. (color online) Radiative shift ($\Delta\hbar\omega$) of resonance peak of optical force versus the QWNS width (L) for p- and s-polarizations, respectively.

In Fig. 4, we plot the maximum radiation force F_x and F_z at resonance for p-polarized state in panels (a) and (b) and for s-polarized state in panels (c) and (d), versus the incident angle θ. We can find that F_x and F_z show a sensitive dependence on the angle of incidence. In Figs. 4(a) and 4(b), it is not hard to see that both F_x and F_z for p-polarized state increase with the incident angle θ increasing. This is because the z component of the incident field increases with the increase of θ, leading to the increase of the z component of the polarization $\widetilde{\boldsymbol{P}}(z,\omega)$ inside the QWNS, while the quantum-size effect plays an important role in the z direction. When $\theta = 90°$, i.e., the incident light is horizontally incident on the QWNS slab, the electronic polarization direction parallels completely to the z direction, which induces F_x and F_z at resonance to be maximum due to the quantum-size effect. However, if $\theta = 0°$, that is, the incident light is perpendicularly incident on the QWNS, the electronic polarization is parallel to the x direction, therefore F_z at resonance is very small because the quantum-size effect does not play any role in this direction, which is the same as that for s-polarized state. In addition, for the two kinds of polarized states, $F_x = 0$ when $\theta = 0°$, because the incident light is perpendicularly incident on the QWNS. From Figs. 4(c) and

4(d), it can be seen that for *s*-polarized state F_x increases and F_z decreases with an increase of the incident angle θ. This is because that the x component of wave vector will increase and its z component will decrease with increasing the incident angle, respectively. In addition, the maximum resonant radiation forces for *p*-polarized state are about six orders of magnitude larger than those for *s*-polarized state, excepting the case of closely perpendicular incidence. The reason is that there exists generally the quantum-size effect for the *p*-polarized state, while it plays no role for the *s*-polarized state. From Fig. 4, we can also see that with increasing the width of the quantum well nanostructure both F_x and F_z for the *p*-polarized state decrease, whereas they increase for the *s*-polarized state when the incident angle θ is fixed. The results obtained in the present paper provide a more quantitative understanding of the nonlocal optical response of nanostructures and the influence of the nonlocality of materials on optical force exerted on objects at the nanometer length scale.

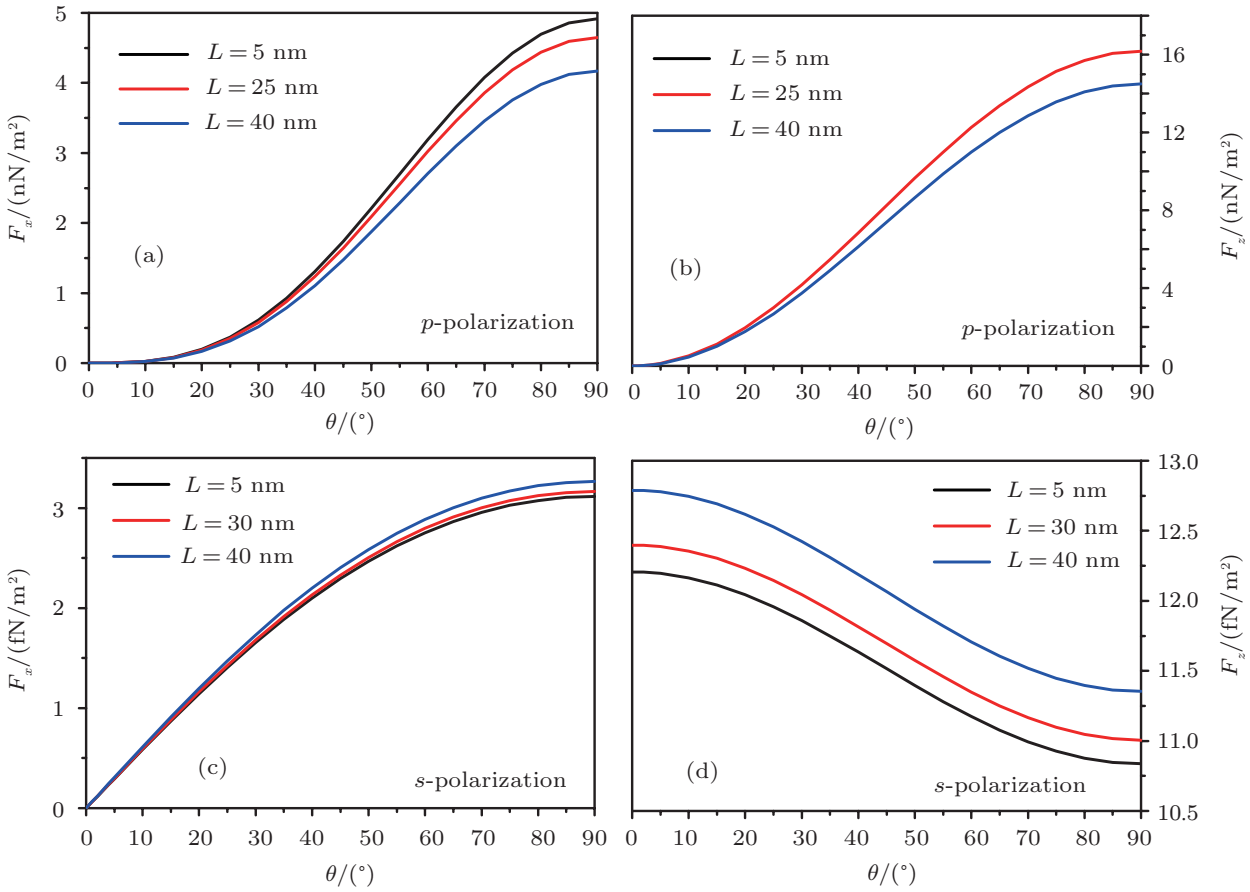


Fig. 4. (color online) Maximum resonant radiation force (F_x and F_z) versus the incident angle θ in the two cases of *p*-polarization [panels (a) and (b)], and *s*-polarization [panels (c) and (d)] for three different QWNS widths, respectively.

4. Summary

In this paper, the nonlocal effects on optical force exerted on the AlGaAs/GaAs QWNS from the resonant intersubband transitions are investigated for two kinds of polarized states, based on the microscopic nonlocal optical response theory. We show that there exists a blueshift of radiation force spectra at resonance induced by the spatial nonlocality of optical response, depending on the QWNS width and the polarization direction. It is also demonstrated that the resonant radiation force is controllable by the QWNS width, the angle of incidence, and the polarization direction of incident light. These properties have potential applications in nano-object manipulation, and have implications for observing radiation forces in experiment. This nonlocal interaction mechanism can also be used to probe and predominate internal quantum properties of nanostructures, and to manipulate collective behavior of nano-objects.

References

[1] Ashkin A, Dziedzic J M, Bjorkholm J E and Chu S 1986 *Opt. Lett.* **11** 288
[2] Chaumet P C, Rahmani A and Nieto-Vesperinas M 2002 *Phys. Rev. Lett.* **88** 123601
[3] Chaumet P C, Rahmani A and Nieto-Vesperinas M 2005 *Phys. Rev. B* **71** 045425
[4] Nieto-Vesperinas M, Sáenz J J, Gómez-Medina R and Chantada L 2010 *Opt. Express* **18** 11428
[5] Wong V and Ratner M A 2006 *Phys. Rev. B* **73** 075416
[6] Iida T and Ishihara H 2007 *Nanotechnology* **18** 084018
[7] Lu J H and Wang G H 2016 *Chin. Phys. B* **25** 117804

[8] Ginis V, Tassin P, Soukoulis C M and Veretennicoff I 2013 *Phys. Rev. Lett.* **110** 057401
[9] Chaumet P C and Nieto-Vesperinas M 2000 *Opt. Lett.* **25** 1065
[10] Li Y and Hu Y J 2013 *Chin. Phys. B* **22** 034206
[11] Liu A and Keller O 1995 *Phys. Scr.* **52** 116
[12] Liu A 1997 *Phys. Rev. B* **55** 7101
[13] Wang G H and Wang R Q 2013 *Appl. Phys. Lett.* **102** 021906
[14] Wang G H, Guo Q, Wu L J and Yang X B 2007 *Phys. Rev. B* **75** 205337
[15] Wang C Y and Wang G H 2014 *Chin. Phys. B* **23** 127103
[16] Chang R and Leung P T 2006 *Phys. Rev. B* **73** 125438
[17] McMahon J M, Gray S K and Schatz G C 2009 *Phys. Rev. Lett.* **103** 097403
[18] Pekar S I 1958 *Eksp Zh. Teor. Fiz.* **34** 1176
[19] Cho K 2003 *Optical Response of Nanostructures: Microscopic Nonlocal Theory* (Berlin: Springer-Verlag) pp. 1–32
[20] Belov P A, Marqués R, Maslovski S I, Nefedov I S, Silveirinha M, Simovski C R and Tretyakov S A 2003 *Phys. Rev. B* **67** 113103
[21] Ishihara H, Cho K, Akiyama K, Tomita N, Nomura Y and Isu T 2002 *Phys. Rev. Lett.* **89** 017402
[22] Luukkonen O, Alitalo P, Costa F, Simovski C, Monorchio A and Tretyakov S 2010 *Appl. Phys. Lett.* **96** 081501
[23] Castaldi G, Galdi V, Alù A and Engheta N 2012 *Phys. Rev. Lett.* **108** 063902
[24] Moreau A, Ciracı C and Smith D R 2013 *Phys. Rev. B* **87** 045401
[25] Luo Y, Fernandez-Dominguez A I, Wiener A, Maier S A, and Pendry J B 2013 *Phys. Rev. Lett.* **111** 093901
[26] Jackson J D 1999 *Classical Electrodynamics* (New York: Willey) p. 3
[27] Zeng J Y 1997 *Quantum Mechanics* (Beijing: Science Press) pp. 74–93